Polycyclic Aromatic Hydrocarbons

DOI: 10.1002/anie.201403227

Synthesis and Properties of a New Class of Fully Conjugated Azahexacene Analogues**

*Wan Yue, Sabin-Lucian Suraru, David Bialas, Matthias Müller, and Frank Würthner**

Dedicated to Professor Fritz Vögtle on the occasion of his 75th birthday

Abstract: *Acenes are a traditional class of polycyclic aromatic hydrocarbons (PAHs) which attracted considerable interest during the last decade because of their outstanding p-channel semiconductor properties. More recently, N-heteroacenes have been prepared. These molecules have been shown to be more stable and can exhibit n-channel semiconductor properties. Inspired by these archetype PAHs, we synthesized a novel class of highly persistent azahexacene analogues* ***3a–d****. These molecules are composed of a core of four fused five-membered rings derived from their respective diketopyrrolopyrroles. These new π-conjugated scaffolds show broad and intense absorption in the visible region and possess low-lying HOMO and LUMO levels, leading to much better stability compared to that of acenes and most heteroacenes.*

Conjugated polycyclic hydrocarbons have attracted considerable attention in the past years as organic electronic materials for various applications, for example, in field-effect transistors, photovoltaics, and light-emitting diodes.[1] Among those polycyclic systems, acenes such as pentacene (**I** in Scheme 1) and its derivatives (e.g. **II**) are prominent examples of semiconducting materials for device applications.[2] However, these systems are susceptible to oxidative and photolytic degradation.[3] According to Clar's sextet rule, as the length of the acene increases, the stability (as well as the solubility) significantly decreases,[4] which causes challenges and difficulties in the synthesis of their higher homologues. Hence our knowledge of acenes longer than pentacene is still limited.[5] The extended polyacene hexacene (**III**) was found to be very unstable in solution, presumably because of its higher reactivity towards dimerization and oxidation.[6] Thus, acene-like topologies such as indeno[1,2-*b*]fluorene skeleton (**IV** in Scheme 1) which with a 6-5-6-5-6 fused ring system in its fully conjugated state closely resembles pentacene, have recently been introduced.[7] An alternative strategy is the incorporation of heteroatoms in the acene framework. In particular, nitrogen-annulated heteroacenes have been shown to be promising electronic materials.[8] For example, triisopropylsilylethyne-functionalized tetraazapentacene (**V**) was shown to be one of the most efficient electron-transport materials in thin-film transistors.[8a] These developments have inspired us to design and synthesize new azaacene-type scaffolds with good stability and solubility as potential electronic materials.

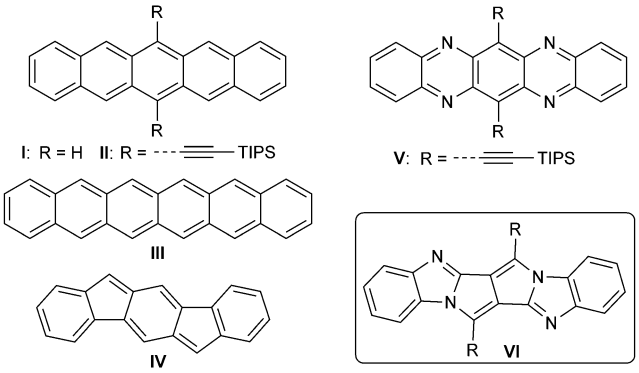

Scheme 1. Chemical structures of pentacene (**I**), bis(triisopropylsilylethynyl)pentacene (**II**),[2e] hexacene (**III**), indeno[1,2-*b*]fluorene (**IV**), bis(triisopropylsilylethynyl)tetraazapentacene (**V**),[8a,g] and our newly designed 6-5-5-5-5-6 fused ring scaffold (**VI**, for substituents R see Scheme 2). TIPS = triisopropylsilyl.

Herein we present a series of new, stable five-membered-ring-fused, nitrogen-annulated, and fully conjugated azahexacene analogues **3a–d** (Scheme 2), which were synthesized starting from their respective 1,4-dioxopyrrolo[3,4-*c*]pyrrole (DPP) derivatives.[9] The X-ray crystal structure of one of the azahexacene derivatives allowed unambiguous confirmation of the 6-5-5-5-5-6 fused ring system, which in its fully conjugated state resembles azahexacenes. The optoelectronic profiles of these new materials have also been explored.

The synthetic route to the newly designed 6-5-5-5-5-6 fused ring systems is outlined in Scheme 2. We firstly developed the synthesis of compound **3a** as a model system starting from DPP derivative **1a**, which was prepared according to a reported method.[10] In contrast to alkylation, arylation of DPPs is rarely reported.[11] A highly electron-deficient aryl electrophile, 2-fluoro-5-trifluoromethylnitrobenzene, in the presence of potassium carbonate in DMF, was used to N-arylate DPP **1a** directly at the amide position. The reaction afforded 3,6-diphenylbis(2-nitro-4-trifluoromethyl)-1,4-dioxopyrrole[3,4-*c*]pyrrole **2a**. Subsequent reduction with

[*] Dr. W. Yue, Dr. S.-L. Suraru, D. Bialas, M. Müller, Prof. Dr. F. Würthner
Universität Würzburg, Institut für Organische Chemie & Center for Nanosystems Chemistry
Am Hubland, 97074 Würzburg (Germany)
E-mail: wuerthner@chemie.uni-wuerzburg.de

[**] Financial support by the German Ministry of Education and Research (BMBF) for this work within the project POLYTOS (FKZ: 13N10205) in the Leading Edge Cluster "Forum Organic Electronics" is gratefully acknowledged.

Supporting information for this article is available on the WWW under http://dx.doi.org/10.1002/anie.201403227.

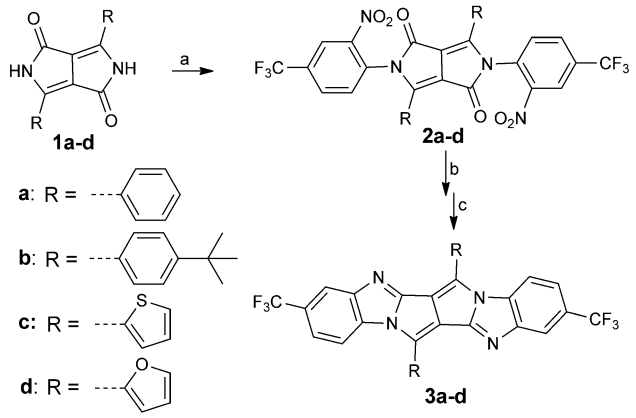

Scheme 2. Synthesis of azahexacene analogues **3a–d**. Reaction conditions: a) 2-Fluoro-5-trifluoromethylnitrobenzene, K_2CO_3, DMF, 70 °C. Yields: **2a** 53%, **2b** 50%, **2c** 54%, **2d** 57%. b) $SnCl_2{\cdot}2H_2O$, ethyl acetate, reflux. c) $TiCl_4$, 1,4-diazabicyclo[2.2.2]octane, mesitylene, 120–125 °C. The overall yields from **2** to **3**: **3a** 15%, **3b** 14%, **3c** 20%, **3d** 17%.

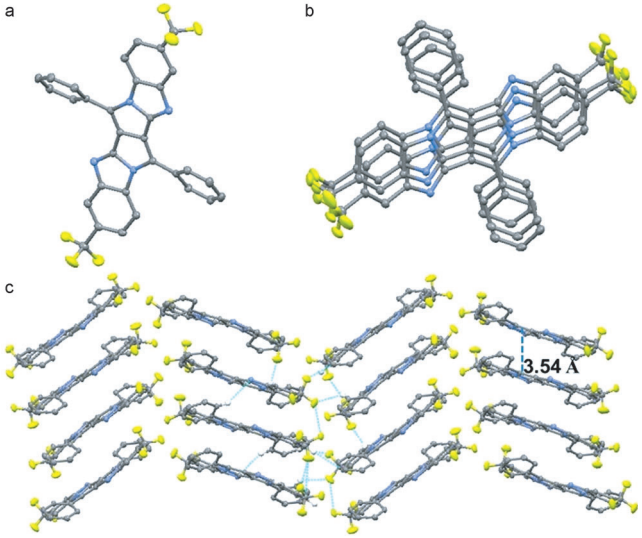

Figure 1. Molecular structure and packing of compound **3a** in the solid state according to single-crystal X-ray analysis. a) Molecular structure; b) overlap between neighboring molecules along the *b*-axis; c) slipped packing motif with interactions between neighboring molecules. Hydrogen atoms are partially omitted for the clarity.

tin chloride dihydrate in ethyl acetate afforded the corresponding diamino-DPP;[12] however, the low solubility and high polarity made the purification of this product difficult. This intermediate was used without further purification in a subsequent intramolecular condensation reaction[13] in the presence of titanium tetrachloride and 1,4-diazabicyclo-[2.2.2]octane (DABCO) in mesitylene. This reaction afforded the desired fully conjugated azahexacene analogue **3a**. The method developed for **3a** was successfully extended to synthesize derivatives **3b–d**, which are disubstituted with a variety of donor (hetero)aromatic moieties, starting from the respective DPPs **1b–d** (Scheme 2). The incorporation of donor groups such as thiophene (**3c**) and furan (**3d**) not only have a strong influence on their optical and electronic properties, but also provide scope for further derivatization.[14,15]

Compound **3a** with two phenyl groups is moderately soluble, and compound **3b** with two 4-*tert*-butylphenyl groups has good solubility in common organic solvents (e.g. chloroform, THF, toluene). Thiophene- and furan-functionalized compounds **3c** and **3d** are soluble in warm organic solvents. Compounds **3a–d** were characterized by high-resolution mass spectrometry (HRMS), and room-temperature or high-temperature ^{1}H NMR and ^{13}C NMR spectroscopy. Compound **3a** was also characterized by single-crystal X-ray analysis. Note, the ^{1}H NMR spectra of precursor compounds **2a–d** (see the Supporting Information) indicate the presence of two isomers as a result of hindered rotation about the C–N bond at the amide positions.

To further confirm the structures of these novel extended π-scaffolds and study the arrangement in the solid state, attention was focused on the growth of single crystals. Crystals of **3a** suitable for X-ray diffraction analysis were obtained by slow evaporation of a dichloromethane/methanol solution of this compound. The molecular structure and crystal packing arrangements are depicted in Figure 1 (for crystallographic data see the Supporting Information).[16] The core skeleton of **3a** is almost planar and the slight distortion might be influenced by the molecular packing in the crystal. As a result of the strong π–π interactions between the large aromatic cores, the molecules are arranged in stacks along the *b*-axis (Figure 1 b). Strong π–π interactions and intermolecular C–H···π interactions drive the arrangement of the molecules into dimers, which are packed tightly in a herringbone fashion with a plane-to-plane distance of approximately 3.54 Å. Additional short contacts C–H···N are evident between the nitrogen atoms in the five-membered rings and the hydrogen atoms on the phenyl ring of the adjacent molecule; the shortest such contact measures 2.69 Å.

The optical properties of new compounds **2a–d** and **3a–d** were studied by UV/Vis absorption spectroscopy (see Figure S1 in the Supporting Information for the spectra of **2a–d**). The spectra of **3a–d** are shown in Figure 2 along with the computed (B3-LYP/6-31 + G*) spectra of compounds **3a** and **3c** at optimized geometries. Compounds **2a–d** and **3a–d** exhibit broad and intense absorption bands in the visible region (Table 1). In contrast with **2a** (λ_{max} = 464 nm) and **2b** (λ_{max} = 483 nm), the absorption maxima of **3a** (λ_{max} = 484 nm) and **3b** (λ_{max} = 494 nm) are bathochromically shifted by approximately 20 and 10 nm, respectively. This shift can be attributed to the extended π-conjugation length within molecules **3a** and **3b**. Variation of the aryl substituents at the core position has a notable impact on the absorption profiles of the compounds. The absorption maxima of thiophene- and furan-substituted derivatives **3c** and **3d** are further bathochromically shifted to λ_{max} = 527 nm and λ_{max} = 570 nm, respectively.

The DFT(B3-LYP/6-31 + G*)-computed absorption spectra of **3a** and **3c** are in good agreement with the experimental spectra and the absorption maxima in the visible region match the experimental data (Figure 2). The HOMOs of compounds

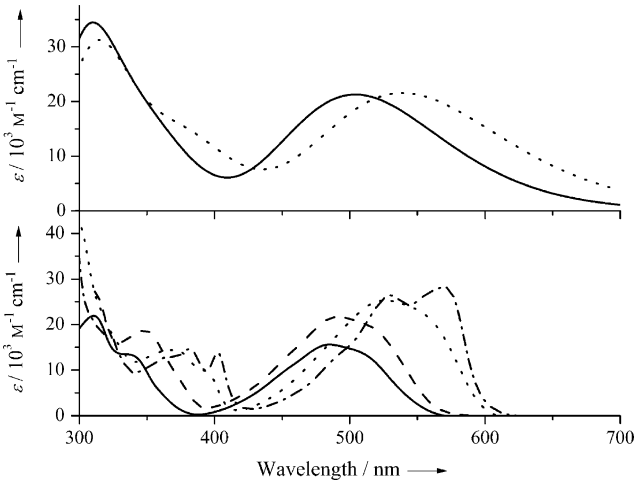

Figure 2. Bottom: UV/Vis absorption spectra of **3a** (solid line), **3b** (dashed line), **3c** (dotted line), and **3d** (dash-dotted line) in chloroform at room temperature. Top: The corresponding DFT(B3-LYP/6-31+G*)-computed spectra of **3a** (solid line) and **3c** (dotted line; top) for comparison.

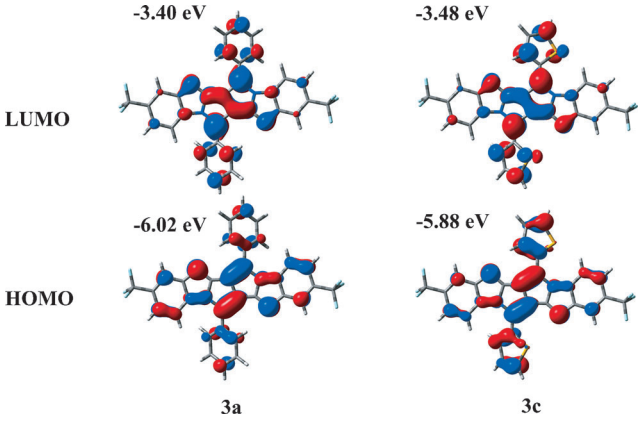

Figure 3. Energies and shapes of DFT(B3-LYP/6-31+G*)-calculated frontier orbitals (HOMOs and LUMOs) of **3a** (left) and **3c** (right).

3a and **3c** are delocalized over the whole annulated π-system, whereas the LUMOs are localized on the four fused five-membered-ring scaffold, including the phenyl and thiophene substituents (Figure 3). It follows from the calculations that the transition from the ground to the first excited states in both compounds is mainly dominated by a HOMO–LUMO transition (for details see Figure S4 and Tables S1 and S2 in the Supporting Information).

Cyclic voltammetry data for compounds **2a–d** and **3a–d** (see Figures S2 and S3) are compiled in Table 1 (the half-wave potential ($E_{1/2}$) for reversible waves or the peak potential (E_p) for irreversible waves are shown). In solution, compounds **2a–d** exhibit one irreversible reduction wave and one or two (see Figure S2) reversible oxidation waves. Molecules **3a–d** with extended π-scaffolds exhibit reversible reduction behavior, accepting one electron with an $E_{1/2}$ value around −1.3 V versus Fc/Fc^+ ($Fc=[(\eta\text{-}C_5H_5)_2Fe]$). Compounds **3a–d** exhibit one irreversible oxidation wave. Substitution with increasingly electron-donating groups induces a shift of the oxidation potentials to less positive values of +0.99, +0.96, +0.84, and +0.72 V for **3a–d**, respectively (Table 1). On the basis of the experimental values, the HOMO energy levels of **3a–3d** are estimated as −5.79, −5.76, −5.64, and −5.52 eV, respectively. Thus, the electron-donating character of the 2-furyl and 2-thienyl groups in **3c** and **3d** leads to an increase in the HOMO energy value compared to that of the phenyl-substituted derivative **3a**, while the LUMO energy is barely affected. The resulting smaller HOMO–LUMO gap explains the bathochromic shift in the absorption spectra of compounds **3c** and **3d**. The electrochemical HOMO–LUMO gaps are also in good agreement with the energy gaps calculated from the absorption spectra (Table 1), which are in agreement with the DFT calculations.

The relative stability of molecule **3a** was examined by UV/Vis spectroscopy under similar conditions as those reported by Miller and co-workers.[3a] No degradation of the compound was observed after four days under ambient air and light conditions (Figure S5). Furthermore, these new molecules are stable upon heating (at 70 °C) for prolonged periods, as required for their ^{13}C NMR spectroscopic measurements, without noticeable decomposition. In contrast, the degradation of pentacene derivatives has been reported after 12 h even at room temperature.[3a]

In summary, we have demonstrated a facile synthetic approach to a new family of fully conjugated nitrogen-annulated 6-5-5-5-5-6 fused ring systems. These new compounds have broad and intense absorption in the visible region, exhibit electron-accepting ability, and have relatively low-lying HOMO and LUMO energy levels. By X-ray crystallographic analysis, **3a** was shown to pack tightly in

Table 1: Optical and electronic properties of compounds **2** and **3**.

Comp.	λ [nm][a]	ε [$M^{-1}cm^{-1}$]	E_{1r} [V][b]	E_{1o} [V][c]	LUMO [eV][d]	HOMO [eV][e]	E_g [eV][f]	E_g [eV][g]
2a	464	23 800	−1.43*	1.04	−3.37	−5.84	2.47	2.42
2b	483	29 600	−1.53*	0.94	−3.27	−5.74	2.47	2.39
2c	537	33 000	−1.37*	0.76	−3.43	−5.56	2.13	2.22
2d	530	46 700	−1.39*	0.75	−3.41	−5.55	2.14	2.27
3a	484	15 700	−1.31	0.99*	−3.49	−5.79	2.30	2.23
3b	494	24 900	−1.39	0.96*	−3.42	−5.76	2.34	2.20
3c	527	25 500	−1.27	0.84*	−3.53	−5.64	2.11	2.06
3d	570	28 500	−1.27	0.72*	−3.53	−5.52	1.99	2.08

[a] UV/Vis absorption maximum in the visible region in chloroform. [b] Irreversible first reduction wave or the reversible half-wave reduction potential (in V vs. Fc/Fc^+) measured in CH_2Cl_2 with a scan rate of 0.1 Vs^{-1}. [c] The irreversible first oxidation wave or the reversible half-wave oxidation potential. [d] Estimated from the irreversible first reduction wave or the reversible half-potential reduction waves using the equation, LUMO = −4.80 + E_{1r}. [e] HOMO levels were estimated from the irreversible first oxidation wave or the reversible half-potential oxidation waves using the equation, HOMO = −4.80 + E_{1o}. [f] E_g = LUMO-HOMO. [g] E_g values were estimated from the onset of the corresponding absorption spectra ($E_g = 1240/\lambda_{onset}$). *Irreversible first reduction or oxidation wave.

slipped π-stacks in the solid state. In combination, our results indicate that these materials are potential organic semiconductors. They also have several advantages compared with pentacene: they can be easily derivatized, they are environmentally stable, and they have good solubility. Further studies on these novel compounds will investigate their device properties and explore potential additional derivatization.

Received: March 11, 2014
Published online: May 5, 2014

Keywords: acenes · aromaticity · dyes/pigments · fused-ring systems · ring annulation

[1] a) *Functional Organic Materials* (Eds.: T. J. J. Müller, U. H. F. Bunz), Wiley-VCH, Weinheim, **2007**; b) *Organic Light Emitting Device: Synthesis Properties and Applications* (Eds.: K. Müllen, U. Scherf), Wiley-VCH, Weinheim, **2006**; c) *Carbon-Rich Compounds* (Eds.: M. M. Haley, R. R. Tykwinski), Wiley-VCH, Weinheim, **2006**.

[2] a) J. E. Anthony, *Angew. Chem.* **2008**, *120*, 460 – 492; *Angew. Chem. Int. Ed.* **2008**, *47*, 452 – 483; b) C. Reese, Z. Bao, *J. Mater. Chem.* **2006**, *16*, 329 – 333; c) L. B. Roberson, J. Kowalk, L. M. Tolbert, C. Kloc, R. Zeis, X. L. Chi, R. Fleming, C. Wilkins, *J. Am. Chem. Soc.* **2005**, *127*, 3069 – 3075; d) H. Klauk, M. Halik, U. Zschieschang, G. Schmid, W. Radlik, W. Werner, *J. Appl. Phys.* **2002**, *92*, 5259 – 5263; e) J. E. Anthony, J. S. Brooks, D. L. Eaton, S. R. Parkin, *J. Am. Chem. Soc.* **2001**, *123*, 9482 – 9483.

[3] a) I. Kaur, W. Jia, R. P. Kopreski, S. Selvarasah, M. R. Dokmeci, C. Pramanik, N. E. McGruer, G. P. Miller, *J. Am. Chem. Soc.* **2008**, *130*, 16274 – 16286; b) A. R. Reddy, M. Bendikov, *Chem. Commun.* **2006**, 1179 – 1181; c) P. Coppo, S. G. Yeates, *Adv. Mater.* **2005**, *17*, 3001 – 3005; d) A. Maliakal, K. Raghavachari, H. Katz, E. Chandross, T. Siegrist, *Chem. Mater.* **2004**, *16*, 4980 – 4986; e) P. V. Schleyer, M. Manoharan, H. J. Jiao, F. Stahl, *Org. Lett.* **2001**, *3*, 3643 – 3646.

[4] E. Clar, *Ber. Dtsch. Chem. Ges. B* **1942**, *75*, 1330 – 1338.

[5] a) I. Kaur, M. N. Jazdzyk, N. Stein, P. Prusevich, G. P. Miller, *J. Am. Chem. Soc.* **2010**, *132*, 1261 – 1263; b) H. Qu, C. Chi, *Org. Lett.* **2010**, *12*, 3360 – 3363; c) B. Purushothaman, S. R. Parkin, J. E. Anthony, *Org. Lett.* **2010**, *12*, 2060 – 2063; d) I. Kaur, N. N. Stein, R. P. Kopreski, G. P. Miller, *J. Am. Chem. Soc.* **2009**, *131*, 3424 – 3425; e) D. Chun, Y. Cheng, F. Wudl, *Angew. Chem.* **2008**, *120*, 8508 – 8513; *Angew. Chem. Int. Ed.* **2008**, *47*, 8380 – 8385; f) M. M. Payne, S. R. Parkin, J. E. Anthony, *J. Am. Chem. Soc.* **2005**, *127*, 8028 – 8029.

[6] a) R. Mondal, C. Tonshoff, D. Khon, D. C. Neckers, H. F. Bettinger, *J. Am. Chem. Soc.* **2009**, *131*, 14281 – 14289; for experimental and theoretical studies on larger acenes see: b) H. F. Bettinger, *Pure Appl. Chem.* **2010**, *82*, 905 – 915; c) R. Einholz, H. F. Bettinger, *Angew. Chem.* **2013**, *125*, 10000 – 10003; *Angew. Chem. Int. Ed.* **2013**, *52*, 9818 – 9820.

[7] a) D. T. Chase, A. G. Fix, S. J. Kang, B. D. Rose, C. D. Weber, Y. Zhong, L. N. Zakharow, M. C. Lonergan, C. Nuckolls, M. M. Haley, *J. Am. Chem. Soc.* **2012**, *134*, 10349 – 10352; b) D. T. Chase, B. D. Rose, S. P. McClintock, L. N. Zakharow, M. M. Haley, *Angew. Chem.* **2011**, *123*, 1159 – 1162; *Angew. Chem. Int. Ed.* **2011**, *50*, 1127 – 1130; c) D. T. Chase, A. G. Fix, B. D. Rose, C. D. Weber, S. Nobusue, C. E. Stockwell, L. N. Zakharow, M. C. Lonergan, M. M. Haley, *Angew. Chem.* **2011**, *123*, 11299 – 11302; *Angew. Chem. Int. Ed.* **2011**, *50*, 11103 – 11106; d) T. Kawase, T. Fujiwara, C. Kiramura, A. Konishi, Y. Hirao, K. Matsumoto, K. Kurata, T. Kubo, S. Shinamura, H. Mori, E. Miyazaki, K. Takimiya, *Angew. Chem.* **2010**, *122*, 7894 – 7898; *Angew. Chem. Int. Ed.* **2010**, *49*, 7728 – 7732; e) U. L. Zerubba, T. D. Tilley, *J. Am. Chem. Soc.* **2010**, *132*, 11012 – 11014; f) M. Satio, M. Nakamura, T. Tajima, *Chem. Eur. J.* **2008**, *14*, 6062 – 6068.

[8] a) U. H. F. Bunz, J. U. Engelhart, B. D. Lindner, M. Schaffroth, *Angew. Chem.* **2013**, *125*, 3898 – 3910; *Angew. Chem. Int. Ed.* **2013**, *52*, 3810 – 3821; b) Z. Liang, Q. Tang, J. Xu, Q. Miao, *Adv. Mater.* **2011**, *23*, 1535 – 1539; c) C. Wang, Z. Liang, Y. L. Liu, X. Wang, N. Zhao, Q. Miao, W. Hu, J. Xu, *J. Mater. Chem.* **2011**, *21*, 15201 – 15203; d) O. Tverskoy, F. Rominger, A. Peters, H.-J. Himmel, U. H. F. Bunz, *Angew. Chem.* **2011**, *123*, 3619 – 3622; *Angew. Chem. Int. Ed.* **2011**, *50*, 3557 – 3560; e) B. D. Lindner, J. U. Engelhart, O. Tverskoy, A. L. Appleton, F. Rominger, A. Peters, H.-J. Himmel, U. H. F. Bunz, *Angew. Chem.* **2011**, *123*, 8747 – 8750; *Angew. Chem. Int. Ed.* **2011**, *50*, 8588 – 8591; f) A. L. Appleton, S. M. Brombosz, S. Barlow, J. S. Sears, J.-L. Breads, S. R. Marder, U. H. F. Bunz, *Nat. Commun.* **2010**, *1*, 91; g) S. Miao, A. L. Appleton, N. Berger, S. Barlow, S. R. Marder, K. I. Hardcastle, U. H. F. Bunz, *Chem. Eur. J.* **2009**, *15*, 4990 – 4993; h) U. H. F. Bunz, *Chem. Eur. J.* **2009**, *15*, 6780 – 6789; i) S. Miao, S. M. Brombosz, P. R. Schleyer, J. I. Wu, S. Barlow, S. R. Marder, K. I. Hardcastle, U. H. F. Bunz, *J. Am. Chem. Soc.* **2008**, *130*, 7339 – 7344; j) M. Winkler, K. N. Houk, *J. Am. Chem. Soc.* **2007**, *129*, 1805 – 1815; k) M. Tadokoro, S. Yasuzuka, M. Nakamura, T. Shinoda, T. Tatenuma, M. Mitsumi, Y. Ozawa, K. Toriumi, H. Yoshino, D. Shiomi, K. Sato, T. Takui, T. Mori, K. Murata, *Angew. Chem.* **2006**, *118*, 5268 – 5271; *Angew. Chem. Int. Ed.* **2006**, *45*, 5144 – 5147; l) J. Nishida, S. Murai, E. Fujiwara, H. Tada, M. Tomura, Y. Yamashita, *Org. Lett.* **2004**, *6*, 2007 – 2010; m) Q. Miao, T.-Q. Nguyen, T. Someya, G. B. Blanchet, C. Nuckolls, *J. Am. Chem. Soc.* **2003**, *125*, 10284 – 10287; n) F. Wudl, P. A. Kouteins, A. Weitz, B. Ma, T. Strassner, K. N. Houk, S. I. Khan, *Pure Appl. Chem.* **1999**, *71*, 295 – 302.

[9] For other π-extended DPP scaffolds, see: a) M. Grzybowski, E. Glodkowska-Mrowka, T. Stoklosa, D. T. Gryko, *Org. Lett.* **2012**, *14*, 2670 – 2673; b) G. M. Fischer, E. Daltrozzo, A. Zumbusch, *Angew. Chem.* **2011**, *123*, 1442 – 1445; *Angew. Chem. Int. Ed.* **2011**, *50*, 1406 – 1409.

[10] T. Potrawa, H. Langhals, *Chem. Ber.* **1987**, *120*, 1075 – 1078.

[11] R.-L. Riggs, C. J. H. Morton, A. M. Z. Stawin, D. M. Smith, N. J. Westwood, W. S. D. Austen, K. E. Stuart, *Tetrahedron* **2005**, *61*, 11230 – 11243.

[12] F. D. Bellamy, *Tetrahedron Lett.* **1984**, *25*, 839 – 842.

[13] H. K. Hall, Jr., A. B. Padias, P. A. Williams, J.-M. Gosau, H. W. Boone, D.-K. Park, *Macromolecules* **1995**, *28*, 1 – 8.

[14] C. H. Woo, P. M. Beaujuge, T. W. Holcombe, O. P. Lee, J. M. J. Fréchet, *J. Am. Chem. Soc.* **2010**, *132*, 15547 – 15549.

[15] a) A. T. Yiu, P. M. Beasjuge, O. P. Lee, C. H. Woo, M. F. Toney, J. M. J. Fréchet, *J. Am. Chem. Soc.* **2012**, *134*, 2180 – 2185; b) D. Bialas, S.-L. Suraru, R. Schmidt, F. Würthner, *Org. Biomol. Chem.* **2011**, *9*, 6127 – 6132; c) Q. Miao, X. Chi, S. Xiao, R. Zeis, M. Lefenfeld, T. Siegrist, M. L. Steigerwald, C. Nuckolls, *J. Am. Chem. Soc.* **2006**, *128*, 1340 – 1345.

[16] CCDC 990258 (**3a**) contains the supplementary crystallographic data for this paper. These data can be obtained free of charge from The Cambridge Crystallographic Data Centre via www.ccdc.cam.ac.uk/data_request/cif.

